Evaluating Invasive EEG Implantations with Structural Imaging Data and Functional Scalp EEG Recordings from Epilepsy Patients

Anil Palepu[1,3,*], Adam Li[1,3,*], Zachary Fitzgerald[2], Katherine Hu[1], Julia Costacurta[1], Juan Bulacio[2], Jorge Martinez-Gonzalez[2], and Sridevi V. Sarma [1,3]

[1]Institute for Computational Medicine, Biomedical Engineering, Johns Hopkins University, Baltimore, United States
[2]Neurosurgery, Cleveland Clinic, Cleveland, United States
[3]IEEE Member, *First two authors contributed equally.

***Abstract*— Seizures in patients with medically refractory epilepsy (MRE) cannot be controlled with drugs. For focal MRE, seizures originate in the epileptogenic zone (EZ), which is the minimum amount of cortex that must be treated to be seizure free. Localizing the EZ is often a laborious process wherein clinicians first inspect scalp EEG recordings during several seizure events, and then formulate an implantation plan for subsequent invasive monitoring. The goal of implantation is to place electrodes into the brain region covering the EZ. Then, during invasive monitoring, clinicians visually inspect intracranial EEG recordings to more precisely localize the EZ. Finally, the EZ is then surgically ablated, removed or treated with electrical stimulation. Unfortunately success rates average at 50%. Such grim outcomes call for analytical assistance in creating more accurate implantation plans from scalp EEG. In this paper, we introduce a method that combines imaging data (CT and MRI scans) with scalp EEG to derive an implantation distribution. Specifically, scalp EEG data recorded over a seizure event is converted into a time-gamma frequency map, which is then processed to derive a spectrally annotated implantation distribution (SAID). The SAID represents a distribution of gamma power in each of eight cortical lobe/hemisphere partitions. We applied this method to 4 MRE patients who underwent treatment, and found that the SAID distribution overlapped more with clinical implantations in success cases than in failed cases. These preliminary findings suggest that the SAID may help in improving EZ localization accuracy and surgical outcomes.**

I. Introduction

Over 60 million people worldwide have epilepsy, and approximately 30% have medically refractory epilepsy (MRE) in that their seizures cannot be controlled by drugs [3]. For focal MRE patients, seizures originate in the epileptogenic zone (EZ), which is the minimum amount of cortex that needs to be treated in order to eliminate seizures [16], [20]. Treatments for focal MRE include, surgical resection of the EZ, laser ablation of the EZ, or stimulation of the EZ. In order for any of these treatments to work, clinicians must successfully localize the EZ. The localization process entails (i) obtaining scalp EEG recordings and imaging data from a patient over several seizure events, (ii) formulating a hypothesis of where the EZ is (both in hemisphere, lobe and/or structures), and then if required, (iii) implanting electrodes either at the surface of the cortex or deep in the brain to cover the hypothetical EZ region. Clinicians then visually inspect the intracranial EEG (iEEG) recordings over several seizure events to precisely localize the EZ. Despite this lengthy monitoring process and despite the fact that large brain regions may be removed, surgical success rates vary between 30%-70% [5], [23].

Such variable outcomes are often due to challenging cases where no lesions appear on MRI scans. In these cases especially, failed treatment may be partially attributed to incorrect or insufficient invasive electrode coverage. With the boom of big data and increased computational power, computational models should be used to assist clinicians in forming an implantation plan from scalp EEG recordings. There are many algorithms that operate on scalp EEG to help localize the EZ [1], [2], [22]. They directly try to predict the region of the EZ, but scalp EEG is insufficient to localize deeper structures that may be involved in seizure events [19]. These approaches do not directly align with how clinicians currently use scalp EEG and imaging data, which is to form an implantation hypothesis (i.e. which lobes to insert iEEG electrodes) for subsequent invasive monitoring.

In this study, we develop an computational approach to assist clinicians in forming an implantation hypothesis from scalp EEG and structural imaging data. Our method processes a patient's scalp EEG recordings over seizure events into a spatio-temporal gamma map, which is then converted into a spectrally annotated implantation distribution (SAID). The SAID quantifies the power in the gamma band over a seizure event in each of eight hempishere-lobe partitions (HLPs) of the brain: Left/Right Frontal (LF, RF), Left/Right Parietal (LP, RP), Left/Right Occipital (LO, RO), Left/Right Temporal (LT, RT). In addition to the patient's T1 MRI and CT scans to generate a clinically annotated implantation distribution (CAID). We applied our method to data from 4 MRE patients treated at the Cleveland Clinic (CC), and each SAID was compared to the CAID by computing the Wasserstein distance (see figure 1). We found that the SAID and CAID are more similar in patients who had successful

A. Li, A. Palepu, S. Sarma are with the Department of Biomedical Engineering, Johns Hopkins University, Baltimore, MD, 21218 USA email correspondence: (adam2392@gmail.com, ssarma2@jhu.edu).

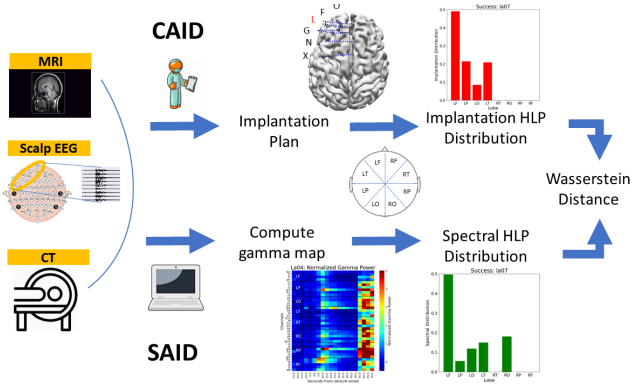

Fig. 1: Analysis pipeline for generating SAID and CAID, where the clinicians produce data to form the CAID and a spectral model of the scalp EEG produces the SAID.

surgical outcomes and less similar in patients who had failed surgical outcomes. These preliminary findings suggest that the SAID may be helpful in formulating iEEG implantations.

II. METHODS

A. Epilepsy Patient Data - Scalp EEG, T1 MRI, CT

The patients included in this study were surgically treated for drug-resistant seizures at the CC. All underwent invasive presurgical monitoring with depth electrodes for seizure localization or mapping of eloquent areas. The number and location of implanted SEEG electrodes are pre-operatively planned based on a pre-implantation hypothesis, which is formulated in accordance with non-invasive pre-implantation data. Decisions regarding the need for invasive monitoring and the placement of electrode arrays were made independently of this work and solely based on clinical necessity. The research protocol was reviewed by the Institutional Review Board (IRB) at the CC.

Pre-operative MRI scans (contrasted with Multihance, 0.1mmol kg^{-1}) were obtained prior to electrode implantation for use in the electrode placement procedure. CT scans were performed after electrode implantation in order to ensure accurate placement and labeling. T1 and CT data was processed using FreeSurfer, FSL and Fieldtrip Toolbox [9], [12], [18]. Scalp EEG recordings were initially acquired with Nihon Kohden system (Nihon Kohden Corp.) with 200Hz sampling rate. Data were then retrospectively obtained for review and converted to EDF format for deidentification and assigned study numbers (e.g. la05), which were then given to us for processing in no specific order. Board-certified electroencephalographers marked, by consensus, the unequivocal electrographic onset of each seizure and the period between seizure onset and termination. Data was then preprocessed as .fif and .json files for analysis in Python with data I/O facilitated by MNE-Python [11].

B. Computing the SAID from Scalp EEG

All data underwent digital filtering with a butterworth notch filter of order 4, with frequency ranges of 59.5 to 60.5. We applied a common average referencing scheme to the data before analysis [17]. This has been shown to produce more stable results and rejects correlated noise across many electrodes [10]. We made sure to exclude any electrodes from subsequent analysis if they were informed to have artifacts in their recording by clinicians. We then considered the discrete fourier transform (DFT) (eq 1), which breaks down a electrode signal, x_n with n as the index through samples of the signal, into its sinusoidal components with certain magnitude and phase [4].

$$X_k = \sum_{n=0}^{N-1} x_n e^{-j\omega_k n} \; k = 0, 1, ..., N-1 \qquad (1)$$

This generates the relative contribution of each frequency component at each point in time for every electrode. We then represent each electrode's DFT in terms of its frequency bands, where we defined the gamma band as 30-100 Hz. We compute the averaged power in the gamma band for each electrode into a gamma map, G. Then for each electrode and its gamma band, we select a baseline as the preictal data for that patient. We then take a selected window of 10-25 seconds after clinically annotated seizure onset ($[W_1, W_2]$) and z-normalize the computed gamma power with respect to the baseline.

In the scalp EEG, we can discretize the contacts into eight regions, or eight hemisphere-lobe partition (HLPs) of the brain for left and right hemispheres: Frontal (LF, RF), Temporal (LT, RT), Parietal (LP, RP) and Occipital (LO, RO) lobes. It is worth noting again that scalp EEG is insufficient to record signals from deeper structures, such as the limbic, or insular regions [19]. So we mainly focus on the cortical surface lobe partitions of the brain. From this data, we can compute an HLP distribution by taking the mean normalized gamma power across all electrodes and selected times in each lobe to calculate the mean power of each lobe in the selected window. These 8 mean power values together will form the SAID for a specific patient.

C. Computing the CAID of SEEG Contacts

We aim to compare the SAID with actual clinical implantations. In order to localize the iEEG contacts in T1 MRI brain space, we first localize the contacts in their CT image, apply an affine transformation to map these coordinates into T1 space, then apply a segmentation algorithm to map each voxel in the T1 image to a brain region, and finally apply a dictionary mapping of each brain region to a lobe (see figure 2). We localize the contacts in the CT image using open-source software from the Fieldtrip Toolbox [18]. Contacts with their corresponding xyz coordinates in the CT image volume are obtained and then mapped to the T1 MRI image volume space via an affine transformation computed by the open-source software FSL [12].

In order to make sense of the SEEG coordinates in the T1 MRI brain space, we perform automated segmentation and parcellation of the T1 MRI image volume using FreeSurfer [9]. This segments the brain into the Desikan-Killany (34 cortical regions per hemisphere) [7], which assigns each voxel

to an annotated brain region. We then apply a dictionary mapping that assigns each of these unique brain regions to a specific lobe as was done with the scalp EEG data. Given the centroid coordinates of each atlas brain region, we apply a nearest-neighbor algorithm to assign each SEEG contact to its nearest brain region. Then, we use the dictionary mapping of these regions to assign the contact to a specific brain lobe. Depending on the contact's hemisphere, if a result is in the Frontal, Temporal, Parietal, or Occipital lobes, we assign the contact to its corresponding HLP lobe. Results in the Limbic or Insular lobes are omitted, as they are not easily assigned to 1 of the 8 HLP lobes. These 8 hemisphere/lobe SEEG contact assignments form the CAID for the patient. In order to quantitatively compare the SAID to the CAID, compute the Wasserstein distance metric between the two. Our code that describes this entire pipeline is available online at: `https://github.com/adam2392/neuroimg_pipeline`.

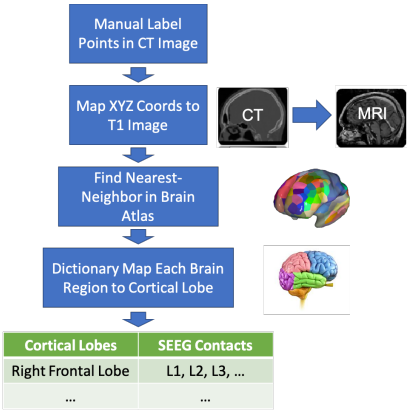

Fig. 2: Outline of how the clinical HLP is computed.

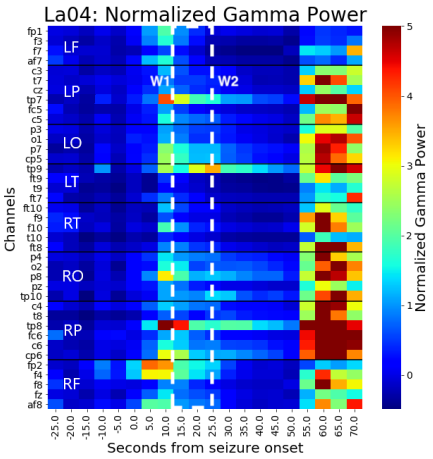

Fig. 3: An example of the normalized gamma power for patient LA04, with hypothesized left-frontal lobe epilepsy. Note that this patient had a failed surgical outcome, indicating that the localization of the EZ failed. The white dashed lines show the selected windows of time used to compute $\tilde{G}$.

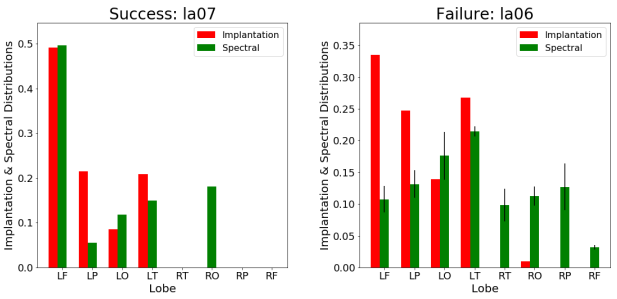

(a) Successful outcome patient's CAID vs SAID for each lobe.

(b) Failed outcome patient's CAID vs SAID for each lobe.

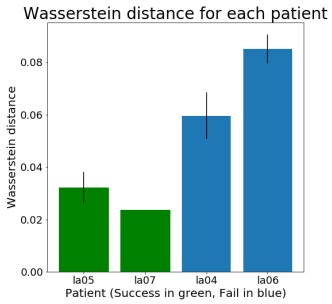

(c) Patient summary (n=4) of CAID vs SAID Wasserstein distance.

Fig. 4: Shows an example of a successful (a) and failed (b) surgical outcome patient's CAID vs SAID distributions and their computed Wasserstein distance between the CAID and SAID for four patients (c). LA07 only had one seizure event, so there are no standard error bars.

III. Results

In this section, we show results of our proposed methodology applied to 4 patients with SEEG implanted. We apply the DFT algorithm to sliding windows of data around the seizure onset, and compute the power within the gamma band. In figure 3, we show an example of the gamma power around seizure onset that is normalized against a preictal baseline. As seen in other studies, we expect a baseline shift in gamma power that is related to a seizure starting [21]. In figure 3, we see that the shift in gamma power does not correspond to the implantation plan for this patient, which is a possible reason for failed treatment of the EZ (i.e. the invasive implantation was not correct).

We then compute the corresponding HLP distributions for each patient and compare to the SAID using the Wasserstein distance. In figure 4, the CAID is more similar to the SAID for successful outcomes. In two of the successful patients, we see a lower Wasserstein distance between the SAID and CAID, while we see a higher distance in failure patients. An example of CAID and SAID for two patients is shown in figure 4a and 4b with the resulting Wasserstein distances shown in figure 4c.

IV. Discussion

In this study, we examine a quantitative method for comparing spectral power in scalp EEG to clinical iEEG

implantations. We do this by defining the contact locations in brain space for a patient through their T1 MRI and CT data and computing the CAID Applying a gamma power spectral model to the data, we can then compute the SAID. We demonstrate that the SAID could potentially be used as a metric for planning implantation distributions. In our preliminary study on four patients, we show that the CAID is more similar to the SAID in successful surgical outcomes, while being more dissimilar in failed surgical outcomes.

Although the method we propose is a quantitative representation of clinical procedure, there are some limitations to the study. Firstly, scalp EEG is insufficient to localize deeper structures such as insular, or limbic regions. A potential way to augment this approach is with diffusion-MRI, which can give insight into structural connections of the brain. We could use this data to infer necessary implantations into deeper regions of the brain. In addition, error is introduced by the variability in resolution for both the T1 and CT images per patient. Furthermore, the seizure onset marked by clinicians is not necessarily when the brain has actually started seizing, especially in cases where the seizure onset is deep below the cortical surface (i.e not directly recordable by scalp EEG). Because a fixed window around seizure onset is always used, the characteristics of the data used to compute power in the gamma band could vary between different patients and seizure events depending on this time delay.

Our framework can be extended further by allowing flexibility in the choice of brain atlas [8], segmentation algorithm [9], and coregistration algorithm [12]. In addition, this framework is not limited to a spectral model of the data. In theory, any model that is applied on the scalp EEG contacts can be used, such as models that include other frequency bands [1], [6], measures of stability [14], personalized whole-brain models [13], [15], or measures of graph statistics [6]. Future work will include analyzing a larger cohort of patients and different models of the data.

ACKNOWLEDGMENT

AL is supported by NIH T32 EB003383, NSF GRFP, Whitaker Fellowship and the Chateaubriand Fellowship, and SVS is supported by NIH R21,NS103113.

REFERENCES

[1] Sergiu Abramovici, Arun Antony, Maria Elizabeth Baldwin, Alexandra Urban, Gena Ghearing, Julie Pan, Tao Sun, Robert Todd Krafty, R. Mark Richardson, and Anto Bagic. Features of Simultaneous Scalp and Intracranial EEG That Predict Localization of Ictal Onset Zone. *Clinical EEG and Neuroscience*, 49(3):206–212, may 2018.

[2] L. P. Andrade-Valenca, F. Dubeau, F. Mari, R. Zelmann, and J. Gotman. Interictal scalp fast oscillations as a marker of the seizure onset zone. *Neurology*, 77(6):524–531, aug 2011.

[3] Anne T. Berg. Identification of Pharmacoresistant Epilepsy. *Neurologic Clinics*, 27(4):1003–1013, nov 2009.

[4] E Oran Brigham. The {F}ast {F}ourier Transform. 55(10):1664–1674, 1974.

[5] Juan C. Bulacio, Lara Jehi, Chong Wong, Jorge Gonzalez-Martinez, Prakash Kotagal, Dileep Nair, Imad Najm, and William Bingaman. Long-term seizure outcome after resective surgery in patients evaluated with intracranial electrodes. *Epilepsia*, 53(10):1722–1730, oct 2012.

[6] Samuel P. Burns, Sabato Santaniello, Robert B. Yaffe, Christophe C. Jouny, Nathan E. Crone, Gregory K. Bergey, William S. Anderson, and Sridevi V. Sarma. Network dynamics of the brain and influence of the epileptic seizure onset zone. *Proceedings of the National Academy of Sciences*, 111(49):E5321–E5330, 2014.

[7] Rahul S Desikan, Florent Ségonne, Bruce Fischl, Brian T Quinn, Bradford C Dickerson, Deborah Blacker, Randy L Buckner, Anders M Dale, R Paul Maguire, Bradley T Hyman, Marilyn S Albert, and Ronald J Killiany. An automated labeling system for subdividing the human cerebral cortex on MRI scans into gyral based regions of interest. 2006.

[8] Christophe Destrieux, Bruce Fischl, Anders Dale, and Eric Halgren. Automatic parcellation of human cortical gyri and sulci using standard anatomical nomenclature. *NeuroImage*, 53(1):1–15, oct 2010.

[9] Bruce Fischl, André van der Kouwe, Christophe Destrieux, Eric Halgren, Florent Ségonne, David H Salat, Evelina Busa, Larry J Seidman, Jill Goldstein, David Kennedy, Verne Caviness, Nikos Makris, Bruce Rosen, and Anders M Dale. Automatically Parcellating the Human Cerebral Cortex. *Cortex*, 14:11–22, 2004.

[10] Stephen V. Gliske, Zachary T. Irwin, Kathryn A. Davis, Kinshuk Sahaya, Cynthia Chestek, and William C. Stacey. Universal automated high frequency oscillation detector for real-time, long term EEG. *Clinical Neurophysiology*, 127(2):1057–1066, 2016.

[11] Alexandre Gramfort, Martin Luessi, Eric Larson, Denis A. Engemann, Daniel Strohmeier, Christian Brodbeck, Lauri Parkkonen, and Matti S. Hämäläinen. MNE software for processing MEG and EEG data. *NeuroImage*, 86:446–460, feb 2014.

[12] Mark Jenkinson, Peter Bannister, Michael Brady, and Stephen Smith. Improved optimization for the robust and accurate linear registration and motion correction of brain images. *NeuroImage*, 17(2):825–41, oct 2002.

[13] V. K. Jirsa, T. Proix, D. Perdikis, M. M. Woodman, H. Wang, C. Bernard, C. Bénar, P. Chauvel, F. Bartolomei, F. Bartolomei, M. Guye, J. Gonzalez-Martinez, and P. Chauvel. The Virtual Epileptic Patient: Individualized whole-brain models of epilepsy spread. *NeuroImage*, 145:377–388, 2017.

[14] Adam Li, Sara Inati, Kareem Zaghloul, and Sridevi Sarma. Fragility in Epileptic Networks : the Epileptogenic Zone. In *American Control Conference*, pages 1–8, 2017.

[15] Adam Li, Woodman Marmaduke, Jirsa Viktor, and Sarma Sridevi. 27th Annual Computational Neuroscience Meeting (CNS*2018): Part Two. In *BMC neuroscience*, volume 19, page 65. BioMed Central, oct 2018.

[16] Hans O. Lüders, Imad Najm, Dileep Nair, Peter Widdess-Walsh, and William Bingman. The epileptogenic zone: General principles. *Epileptic Disorders*, 8(SUPPL. 2), 2006.

[17] K. A. Ludwig, R. M. Miriani, N. B. Langhals, M. D. Joseph, D. J. Anderson, and D. R. Kipke. Using a Common Average Reference to Improve Cortical Neuron Recordings From Microelectrode Arrays. *Journal of Neurophysiology*, 101(3):1679–1689, mar 2009.

[18] Robert Oostenveld, Pascal Fries, Eric Maris, and Jan-Mathijs Schoffelen. FieldTrip: Open source software for advanced analysis of MEG, EEG, and invasive electrophysiological data. *Computational intelligence and neuroscience*, 2011:156869, dec 2011.

[19] Steven V. Pacia and John S. Ebersole. Intracranial EEG Substrates of Scalp Ictal Patterns from Temporal Lobe Foci. *Epilepsia*, 38(6):642–654, jun 1997.

[20] W PENFIELD. Epileptogenic lesions. *Acta neurologica et psychiatrica Belgica*, 56(2):75–88, feb 1956.

[21] Liankun Ren, Michal T Kucewicz, Jan Cimbalnik, Joseph Y Matsumoto, Benjamin H Brinkmann, Wei Hu, W Richard Marsh, Fredric B Meyer, S Matthew Stead, and Gregory A Worrell. Gamma oscillations precede interictal epileptiform spikes in the seizure onset zone. *Neurology*, 84(6):602–8, feb 2015.

[22] Willeke Staljanssens, Gregor Strobbe, Roel Van Holen, Vincent Keereman, Stefanie Gadeyne, Evelien Carrette, Alfred Meurs, Francesca Pittau, Shahan Momjian, Margitta Seeck, Paul Boon, Stefaan Vandenberghe, Serge Vulliemoz, Kristl Vonck, and Pieter van Mierlo. EEG source connectivity to localize the seizure onset zone in patients with drug resistant epilepsy. *NeuroImage: Clinical*, 16:689–698, jan 2017.

[23] Vejay N. Vakharia, John S. Duncan, Juri Alexander Witt, Christian E. Elger, Richard Staba, and Jerome Engel. Getting the best outcomes from epilepsy surgery. *Annals of Neurology*, 2018.